Progesterone Increases Rat Neural Progenitor Cell Cycle Gene Expression and Proliferation Via Extracellularly Regulated Kinase and Progesterone Receptor Membrane Components 1 and 2

Lifei Liu, Junming Wang, Liqin Zhao, Jon Nilsen, Kelsey McClure, Karren Wong, and Roberta Diaz Brinton

Program in Neuroscience (L.L., R.D.B.), Department of Pharmacology and Pharmaceutical Sciences (J.W., L.Z., J.N., K.M., R.D.B.), and University of Southern California Science Technology and Research Program (K.W.), University of Southern California, School of Pharmacy Pharmaceutical Sciences Center, Los Angeles, California 90033

Progesterone receptor (PR) expression and regulation of neural progenitor cell (NPC) proliferation was investigated using NPC derived from adult rat brain. RT-PCR revealed that PRA mRNA was not detected in rat NPCs, whereas membrane-associated PRs, PR membrane components (PGRMCs) 1 and 2, mRNA were expressed. Progesterone-induced increase in 5-bromo-2-deoxyuridine incorporation was confirmed by fluorescent-activated cell sorting analysis, which indicated that progesterone promoted rat NPC exit of G_0/G_1 phase at 5 h, followed by an increase in S-phase at 6 h and M-phase at 8 h, respectively. Microarray analysis of cell-cycle genes, real-time PCR, and Western blot validation revealed that progesterone increased expression of genes that promote mitosis and decreased expression of genes that repress cell proliferation. Progesterone-induced proliferation was not dependent on conversion to metabolites and was antagonized by the $ERK_{1/2}$ inhibitor UO126. Progesterone-induced proliferation was isomer and steroid specific. PGRMC1 small interfering RNA treatment, together with computational structural analysis of progesterone and its isomers, indicated that the proliferative effect of progesterone is mediated by PGRMC1/2. Progesterone mediated NPC proliferation and concomitant regulation of mitotic cell cycle genes via a PGRMC/ERK pathway mechanism is a potential novel therapeutic target for promoting neurogenesis in the mammalian brain. **(*Endocrinology* 150: 3186–3196, 2009)**

Emerging data indicate that progesterone (P_4) has multiple nonreproductive functions in the central nervous system (CNS) to regulate cognition, mood, inflammation, mitochondrial function, neurogenesis, regeneration, myelination, and recovery from traumatic brain injury (1–6). As a neurosteroid, P_4 can be generated *de novo* in the CNS (7–9). Developmentally, P_4 is synthesized in the CNS throughout the embryonic period in the pluripotential progenitor cells (10, 11) and reaches its highest concentration in late gestation (12). P_4-regulated neural responses are mediated by an array of progesterone receptors (PRs), including the classic nuclear receptor (cPR) PRA and PRB, the seven-transmembrane domain-β, and the membrane-associated 25-kDa protein (25-Dx) PR membrane components (PGRMCs) 1 and 2 (1).

P_4 can promote cell proliferation in the breast (13–16) and has both inhibitory and stimulatory effects in the uterus, depending on cell type, the regimen of treatment, whether PRA or PRB is expressed, the dose of 17β-estradiol (E_2) and P_4, and when in the cycle P_4 is administered (1). As in the uterus, P_4 regulation of mitosis in the nervous system is complex. Results from multiple laboratories have indicated that P_4 regulates neural cell proliferation in both the peripheral and CNS (17–20). Tanapat *et al.* (21) have shown that ovariectomized rats treated with a high dose of E_2 showed enhanced hippocampal cell proliferation and

ISSN Print 0013-7227 ISSN Online 1945-7170
Printed in U.S.A.

doi: 10.1210/en.2008-1447 Received October 14, 2008. Accepted March 27, 2009.
First Published Online April 9, 2009

Abbreviations: APα, 3α-Hydroxy-5α-pregnan-20-one (allopregnanolone); bFGF, basic fibroblast growth factor; BrdU, 5-bromo-2-deoxyuridine; CDCZ, cell division cycle 2; CDK, cyclin-dependent kinase; CNS, central nervous system; cPR, classic progesterone receptor; C_T, cycle threshold; DAPI, 4′, 6-diamidino-2-phenylindole; E_2, 17β-estradiol; EC_{100}, maximally effective concentration; FACS, fluorescence-activated cell sorting; GABA, γ-aminobutyric acid; NPC, neural progenitor cell; P_4, pregn-4-ene-3, 20-dion (progesterone); PCNA, proliferating cell nuclear antigen; PGRMC, PR membrane component; PR, progesterone receptor; rNPC, rat NPC; siRNA, small interfering RNA.

subsequent exposure to P_4 antagonized E_2-induced enhancement of cell proliferation after an initial increase. Interestingly, previous work from our laboratory demonstrated that 24 h exposure of embryonic d 18 rat hippocampal neurons to P_4 alone induced a 20% increase in [^{3}H]thymidine uptake, a phenomenon similar to that was observed after allopregnanolone (APα) exposure (1), indicating that P_4 alone may promote hippocampal progenitor cell proliferation and thereby act as a neurogenic agent.

Whereas P_4 is well characterized for its neuroprotective effects in the CNS (3, 5, 22–27) and proliferative effects in the breast and uterus (1), knowledge regarding its proliferative capability in the adult CNS, particularly in the neural stem/progenitor cell population, is limited. Thus, the first series of studies were designed to determine the neurogenic potential of P_4 in neural progenitor cells (NPCs) derived from adult rat dentate gyrus using cellular, morphological, biochemical, and genomic approaches. Furthermore, to determine the mechanism underlying P_4's actions, a second series of studies were carried out to investigate signaling pathway and the effect of PGRMC1 small interfering RNA (siRNA) treatment on P_4's effect.

Materials and Methods

Steroids

All steroids used in this study were purchased from Steraloids (Newport, RI). They are: pregn-4-ene-3,20-dione(progesterone), 5α-pregnane-3,20-dione(5α-dihydroprogesterone), 3α-hydroxy-5α-pregnan-20-one (allopregnanolone), 3β-hydroxy-5β-pregnan-20-one(epipreg-nanolone), 3α-hydroxy-5β-preg-nan-20-one(epiallopregnanolone), 3β-hydroxy-5α-pregnan-20-one, 3α-hydroxy-5β-meth-yl-5α-pregnan-20-one(ganaxolone), 5α-pregnan-3β-ol, 5-pregnan-3β-ol-20-one-3-sulfate(pregnanolone sulfate), 5α-pregn-an-3α,20α-diol(allopregnanediol), and 5α-pregnan-3α,17,20α-triol(allopregnanetriol).

Culture of rat NPCs

Rat NPCs derived from adult rat dentate gyrus (gift from Dr. Fred Gage, Laboratory of Genetics, The Salk Institute, La Jolla, CA) were provided as cryopreserved cells. They were cultured as described previously (28, 29) in DMEM/Ham's F-12 medium (1:1; Omega Scientific, Tarzana, CA) with 1% penicillin/streptomycin/amphotericin B (Invitrogen, Grand Island, NY), supplemented with N2 (1%; Invitrogen) and basic fibroblast growth factor (bFGF; 20 ng/ml; Invitrogen) in a humidified incubator (37 C and 5% CO_2). Cells were plated at a density of $2 \times e^6$ cells/flask, $7.5–15 \times e^4$ cells/well of 96-well plates, or $2–4 \times e^4$ cells/cm^2 for chamber slides for analysis.

Immunocytochemical staining

To check the cell composition in the culture, rat NPCs (rNPCs) were plated onto four-well chamber slides and processed as described before (1) with the following primary antibodies (30, 31): monoclonal antibody for neuronal class IIIβ-tubulin (NPC marker, 1:500; Covance Laboratories, Vienna, VA), monoclonal antibody for nestin (1:5000; Chemicon, Temecula, CA), monoclonal antibody for proliferating cell nuclear antigen (PCNA; 1:100; Zymed Laboratories, San Francisco, CA), and polyclonal antibody for PGRMC1 (32, 33), followed by incubation with appropriate secondary antibodies conjugated with fluorescein isothiocyanate (1:200; Vector Laboratories, Burlingame, CA) or Texas Red (1:50; Vector Laboratories). Slides were mounted with 4′, 6-diamidino-2-phenylindole (DAPI)-containing mounting medium (Vector Laboratories), observed by Axiovert 200M fluorescent microscope (Zeiss, Oberkochen, Germany), and images were captured by SlideBook software (Intelligent Imaging Innovations, Denver, CO).

5-Bromo-2-deoxyuridine (BrdU) incorporation

Cell proliferation was evaluated by measuring the incorporation of BrdU in the S phase of the cell cycle. After 4–6 h starvation (medium without supplements), rNPCs were loaded with 10 μM BrdU in the presence or absence of bFGF and a different concentration of P_4 or other steroids in unsupplemented maintenance medium for 1 d. The cells were then processed using the method as described previously (34, 35) with kits purchased from Roche (Penzberg, Germany) and read with an Lmax microplate luminometer (Molecular Devices, Sunnyvale, CA). After subtracting the value of the blank (without BrdU loading), the results were analyzed using a one-way ANOVA, followed by a Neuman-Keuls *post hoc* test and presented as percentage increase *vs.* control.

Fluorescence-activated cell sorting (FACS) analysis

After 4 h of growth factor deprivation and incubation with vehicle ($1 \times e^{-6}$ ethanol) or 100 pM P_4 for indicated time, rNPCs were collected into Falcon 12- × 75-mm tubes (polystyrene). After fixation with 100% ethanol and stained with propidium iodide for nuclear content, the cells were subjected to FACS analysis. In each sample, $1 \times e^5$ cells were counted by LSRII flow cytometer (BD Biosciences, San Jose, CA); the numbers of cells under each phase of cell cycle were obtained, and analyzed using the embedded cell cycle analysis tool of the FlowJo program (Tree Star Inc., Ashland OR).

Gene-array assay

To analyze cell-cycle gene regulation, a commercially available targeted cDNA array of 112 cell-cycle regulatory genes and several housekeeping genes (Oligo GEArray rat cell cycle microarray; SABiosciences, Frederick, MD) was used to analyze cell-cycle gene regulation. After 6 h starvation, rNPCs were treated with or without 100 pM P_4 for 6 h, and total RNA was isolated using TRIzol reagent (Invitrogen) as described by the manufacturer. Ten micrograms of total RNA were reverse transcribed into biotin-16-deoxy-uridine 5-triphosphate-labeled single-strand cDNA and hybridized with nylon membrane, followed by incubation with alkaline phosphate-conjugated streptavidin. Chemiluminescence was visualized and captured by ChemiDoc XRS system (Bio-Rad, Hercules, CA). The intensity of the spots was extracted and data were analyzed using online GEArray expression analysis suite (http://geasuite.superarray.com/). Glyceraldehyde-3-phosphate dehydrogenase and Aldoa were used as internal controls. Bacterial plasmid (pUC18) was used as a negative control.

Real-time RT-PCR

Real-time RT-PCR was performed to validate the gene-array results. Total RNA was prepared as described above. cDNA synthesis and PCR amplification was carried out using iScript one-step RT-PCR kit with SYBR green (Bio-Rad) and primers as described before (34, 35). RT-PCR and melting curve analysis were performed in multiplicate in optimized conditions as described by manufacturer. No other products were amplified because melting curves showed only one peak in each primer pair. Fluorescence signals were measured over 40 PCR cycles and β-actin was used as internal control. The cycle number (C_T) at which the signals crossed a threshold set within the logarithmic phase was recorded and the differences in cycle threshold ($\Delta\Delta C_T$) were used to analyze the gene expression in the P_4- and vehicle-treated group: target $gene_{P4}$/target $gene_{vehicle} = 2^{-\Delta\Delta CT}$, where $\Delta\Delta C_T = (C_{T,\ target\ gene} - C_{T,\ actin})_{P4} - (C_{T,\ target\ gene} - C_{T,\ actin})_{vehicle}$.

Western blot analyses

After 6 h starvation, rNPCs were treated with or without 100 pM P_4 for 10–12 h and processed for Western blot as described before (34, 35). The proliferative effects P_4 were further validated by accessing PCNA and Cell Division Cycle 2 (CDC2) at the protein level. After overnight incubation with monoclonal antibody for PCNA (1:500; Zymed Labo-

ratories) or polyclonal antibody for CDC2 (1:500; Novus Biologicals, Littleton, CO), and PGRMC1 expression levels were determined using polyclonal antibody for PGRMC1 (1:300; Sigma, St. Louis, MO). Membranes were then incubated in horseradish peroxidase-conjugated goat antirabbit or horse antimouse IgG, and results were visualized by the 3′, 5, 5′-tetramethyl benzidine peroxidase substrate kit (Vector Laboratories). Relative amounts of PCNA and CDC2 were quantified by optical density analysis using the UN-SCAN-IT gel automated digitizing system (Silk Scientific, Inc., Orem, UT). The level was normalized with respect to β-actin, and data are presented as mean ± SEM.

Computer modeling

All calculations were performed on a SGI Octane graphical workstation equipped with the IRIX 6.5 operating system (Silicon Graphics Inc., Mountain View, CA). An automated ligand-docking program, GOLD3.0 (Genetic Optimization for Ligand Docking, Cambridge, UK; Cambridge Crystallographic Data Center), was used to predict the binding modes of steroids into cPR binding site as described before (3, 34). The three-dimensional structural coordinate data of human PR-ligand-binding domain complexes with P_4 was obtained from the Protein Data Bank (PDB entry: 1A28). The three-dimensional structures of steroids were constructed and energy minimized using the molecular modeling program InsightII 2000 (Accelrys Inc., San Diego, CA). GOLD offers several fitness functions, and GoldScore, which has been optimized for the prediction of ligand binding positions, was used in the present study.

PR competitive binding

The PR binding affinity and selectivity of the steroids were determined by a fluorescent polarization competitive binding assay using purified baculovirus-expressed human PR and a fluorescent progesterone ligand PL Red (Invitrogen) as described before (3, 34). Polarization values were plotted against the logarithm of the test compound concentration and IC_{50} value, the concentration of the test compound that displaces half of the PL Red from PR, was determined from the plot using a nonlinear least-squares analysis using Origin, version 8 (OriginLab Corp., Northampton, MA). Negative controls containing PR and PL Red (equivalent to 0% inhibition) and positive controls containing only free PL Red (equivalent to 100% inhibition) were included.

PGRMC1 siRNA treatment

Scrambled (catalog no. AM4611) or one of three predesigned PGRMC1 siRNAs (siRNA ID 253163, 253164, and 253165; Ambion, Austin, TX) was mixed with siPORT NeoFX transfection agent (Ambion) to yield a final concentration of 30 nm and siRNA transfection carried out according the siPORT NeoFX protocol outlined by Ambion. PGRMC1 siRNA no. 253163 and 253165 targeted sequences in the noncoding region (nucleotides 977-994 and 1329-1348, respectively). PGRMC1 siRNA no. 253164 targeted the polyA tail of PGRMC1 (nucleotides 1853-1870). After siRNA treatment for 24, 48, and 72 h, rNPCs were collected and processed for both immunocytochemically staining and Western blot analysis for PGRMC1 expression as described earlier. This pilot study revealed that optimal treatment paradigm was PGRMC1 siRNA 253163 for 48 h. For Western blot analysis, rNPCs were transfected with either scrambled or PGRMC1 siRNA 253163 for 48 h; starved for 4 h; treated with bFGF, vehicle, or 100 pM P_4 for 10–12 h; and processed for Western blot analysis for PGRMC1, PCNA, and CDC2 expression level.

Statistical analysis

All experiments were repeated three to four times. When appropriate, data from each replicate were pooled and analyzed by either a Student *t* test if only two treatment groups were involved or by one-way ANOVA followed by Neuman-Keuls *post hoc* analysis if means of three or more groups were compared. Data displayed in graphs were reported as mean ± SEM or fold change ± SEM. $P < 0.05$ was considered to be significant, regardless of the statistical test used.

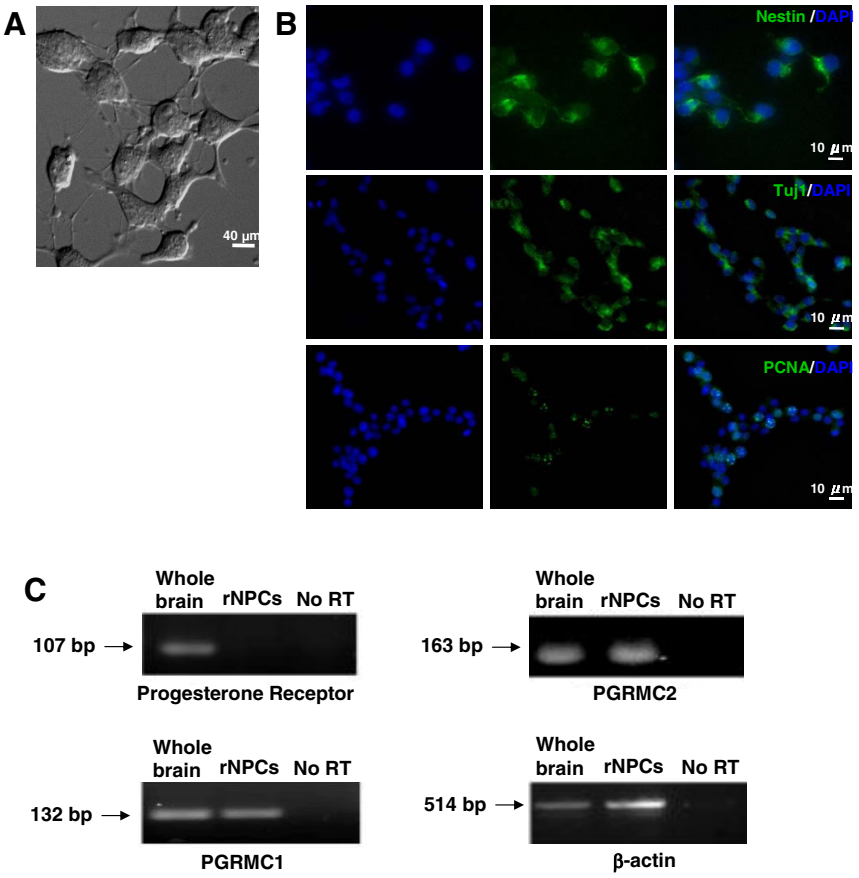

FIG. 1. Characterization of NPCs derived from adult rat dentate gyrus. A, Light microscopy of adult rNPCs. B, Rat NPCs stained for phenotypic markers. *Upper panel*, rNPCs stained for nestin (*green*) and DAPI (*blue*) for nuclei; *middle panel*, rNPCs stained for Tuj1 (*green*) and DAPI (*blue*); *lower panel*, rNPCs stained for PCNA (*green*) and DAPI (*blue*). C, RT-PCR detection of cPR and PGRMC1 and -2 expression in rNPCs. Rat NPCs do not express detectable amounts of cPR RNA, whereas the expression of both PGMRC1 and -2 were shown. A sample without reverse transcriptase (no RT) was used as negative control. β-Actin was used as loading control.

Results

Characterization of NPCs derived from adult rat dentate gyrus

The neural progenitor phenotype of rNPCs (gift of Dr. Fred Gage, Salk Institute, La Jolla, California) was verified by labeling for stem/progenitor cell marker, nestin (30, 34), neural progenitor/neuronal marker, Tuj1 (31, 34), and PCNA, a proliferating cell nuclear antigen associated with transition through S phase (34). Cells were counterstained with DAPI for nuclei. Whereas rNPCs were nestin and Tuj1 positive, only a subset was in an active mitotic stage as indicated by PCNA expression (Fig. 1A), which is consistent with previous reports (28, 29).

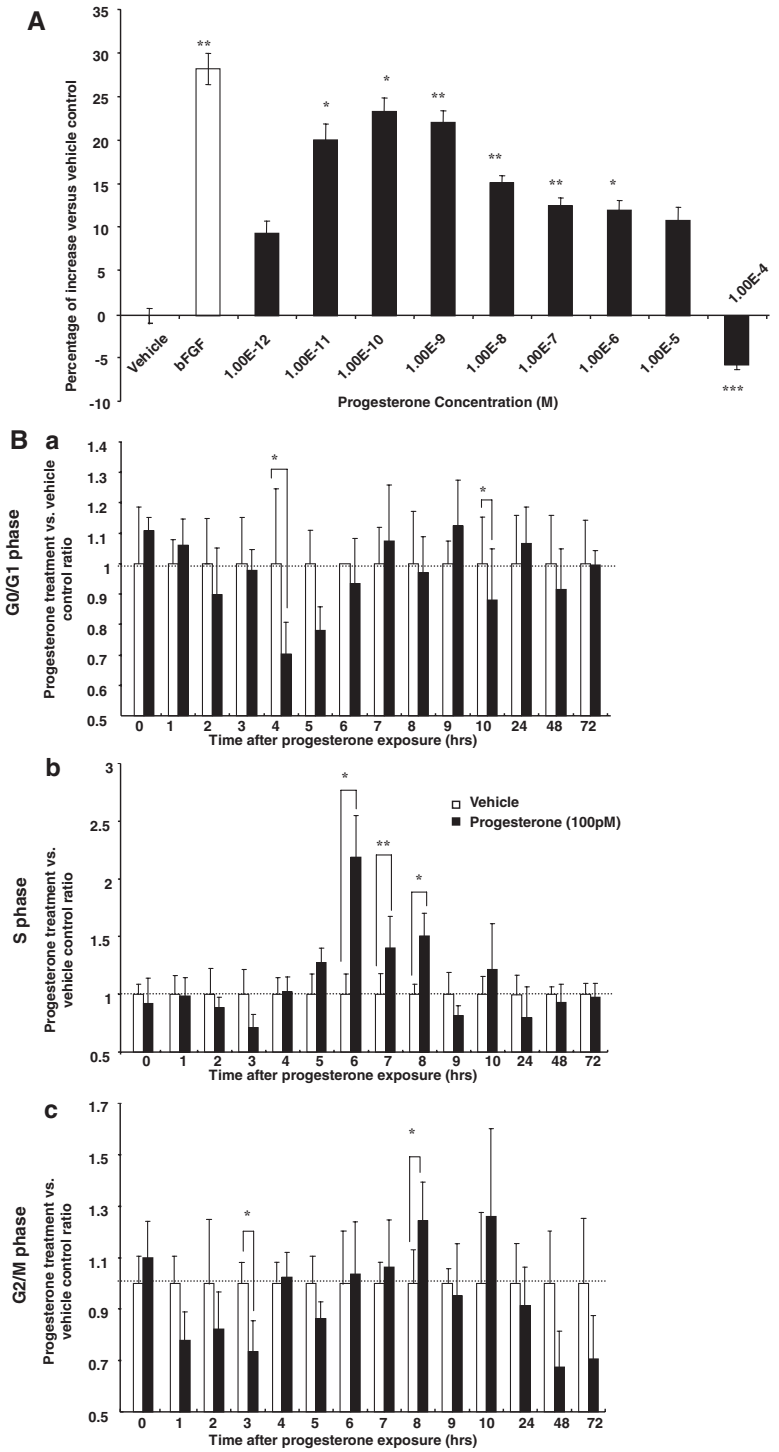

FIG. 2. P_4 promotes rNPC proliferation in a dose- and time-dependent manner. A, Dose response of P_4-induced proliferation in rat NPCs. Rat NPCs were starved for 4 h before treatment of P_4 ($1 \times e^{-12}$ to $1 \times e^{-4}$ M) for 24 h, and cell proliferation was evaluated by BrdU chemiluminescence ELISA measuring BrdU incorporation. Ethanol was used as vehicle control ($1 \times e^{-6}$). P_4-induced cell proliferation showed a dose-dependent manner. Data were collected from three independent assays, analyzed using one-way ANOVA, followed by Neuman-Keuls *post hoc* test, and plotted as percentage increase *vs.* vehicle control. Data are mean ± SEM and vehicle control was set to zero. *, $P < 0.05$ *vs.* control; **, $P < 0.01$ *vs.* vehicle control; ***, $P < 0.001$ *vs.* vehicle control. B, FACS analysis of 100 pM P_4 effect on rNPC cell cycle progression. Rat NPCs were starved for 4 h before treatment of P_4 (100 pM) or vehicle control ($1 \times e^{-6}$ ethanol). Cells were harvested at time points indicated on the x-axis and processed for FACS analysis for DNA content and cell cycle progression. Ba, 100 pM P_4 effect on G_1-phase population; Bb, 100 pM P_4 effect on S-phase population; Bc, 100 pM P_4 effect on G_2/M-phase population. To eliminate the variation introduced by time, at each time point results from both groups were normalized to the vehicle control at the same time point, and vehicle control was set to one. Data were collected from three independent experiments and plotted as percent of rNPCs in each cell cycle in the P_4-treated group *vs.* vehicle control (mean ± SEM). *, $P < 0.05$ *vs.* vehicle control; **, $P < 0.01$ *vs.* vehicle control.

The expression profile of PRs in rNPCs was determined by RT-PCR for cPR, PGRMC1, and PGRMC2. RNA from rat whole brain was used as positive control, and a sample without reverse transcriptase (no RT) was used as a negative control. Results of RT-PCR indicated that both PGRMC1 and -2 were present in rNPCs, whereas cPR was not detectable (Fig. 1B). This finding is consistent with previous reports that cPR is expressed in select cell populations in brain (1, 36).

P_4 promotes rNPC proliferation in a dose-and time-dependent manner

BrdU chemiluminescence cell proliferation ELISA was conducted to determine the dose response and time course of P_4-induced rNPC proliferation. To eliminate the contribution of growth factors in the culture medium, rNPCs were growth factor deprived for 4 h before exposure to P_4 (at concentrations ranging from $1 \times e^{-12}$ to $1 \times e^{-4}$ M), followed by BrdU ELISA. Our preliminary analyses indicated that 4 h starvation ensured sufficient cell synchronization and avoided loss of rNPC proliferative capability. P_4 induced a dose-dependent effect on BrdU incorporation in rNPCs (Fig. 2A) with an maximally effective concentration (EC_{100}) at $1 \times e^{-10}$ M (23.5 ± 1.6% increase *vs.* vehicle, $P < 0.05$), an effect comparable with that induced by bFGF (20 ng/ml, 31.3 ± 1.8% increase *vs.* vehicle, $P < 0.01$). P_4-inducd BrdU incorporation exhibited an inverted-U-shape dose response with a decline in incorporation evident at $1 \times e^{-8}$ M, maximal at $1 \times e^{-5}$ M, and a significant inhibitory effect at $1 \times e^{-4}$ M. The optimal P_4 concentrations for inducing proliferation were $1 \times e^{-11}$ to $1 \times e^{-9}$ M. For subsequent experiments, $1 \times e^{-10}$ M (100 pM) was selected as the P_4 dose unless indicated otherwise.

To verify P_4 regulation on rNPC proliferation, cell cycle entry was analyzed using FACS analysis. After 4 h of growth factor deprivation and exposure to either vehicle or P_4 for indicated time period (Fig. 2B, a–c), rNPCs were collected and labeled with propidium iodide for DNA content analysis. To eliminate variations introduced across time, percent of cells within different cell cycle phases after P_4 exposure was normalized to vehicle control at the same time point and plotted as percent increase relative to con-

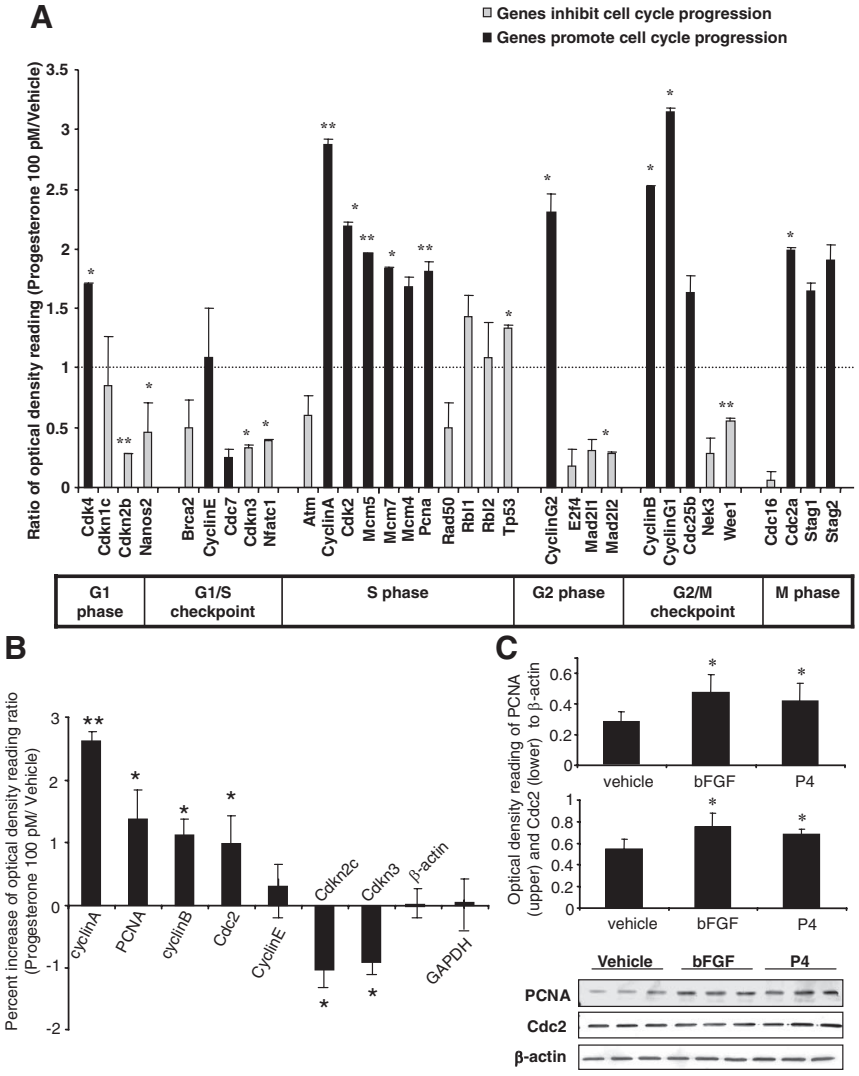

FIG. 3. P_4 regulates cell-cycle gene expression. For gene array analysis, rNPCs were starved for 4–6 h and then treated with vehicle or 100 pM P_4 for 6 h, followed by extraction of total RNA. For Western blot analysis, after 4–6 h starvation, rNPCs were treated with bFGF, vehicle, or 100 pM P_4 for 24 h; collected; and processed for Western blotting. A, RNA was processed for DNA gene array analysis. Changes in gene expressions were grouped according to function. P_4 induced significant increase in genes that promote progression through the cell cycle and inhibited genes associated with exiting the cell cycle (summarized in supplemental Table 1). Two housekeeping genes (Aldoa and glyceraldehyde-3-phosphate dehydrogenase) were used as internal controls. Two blanks and pUC18 from bacterial plasmid were used as negative controls. Data were represented as percent change of mRNA expression in P_4-treated rNPCs *vs.* control (mean ± SEM) as determined by OD. Data were from three separate experiments and analyzed using both multivariant ANOVA statistical analysis and one-way ANOVA, followed by Neuman-Keuls *post hoc* test. *, $P < 0.05$ *vs.* vehicle control; **, $P < 0.01$ *vs.* vehicle control. B, Validation of the gene-array results by real-time RT-PCR. $\Delta\Delta C_T$ was used to analyze the ratio of gene expression in the P_4-treated group and vehicle control as follows: target $gene_{P4}$/target $gene_{vehicle} = 2^{-\Delta\Delta CT}$, where $\Delta\Delta C_T = (C_{T,\ target\ gene} - C_{T,\ actin})_{P4} - (C_{T,\ target\ gene} - C_{T,\ actin})_{vehicle}$. Data are depicted as percent increase of mRNA expression in P_4-treated rNPCs *vs.* vehicle control (mean ± SEM) from three separate experiments. Controls were set to zero and β-actin was used as internal control. *, $P < 0.05$ *vs.* vehicle control; **, $P < 0.01$ *vs.* vehicle control. C, Validation of the gene array results by Western blot analysis of two mitotic markers, PCNA and CDC2. Ethanol was used as vehicle control and bFGF was used as positive control. Data are depicted as percent increase of protein expression in P_4-treated rNPCs *vs.* vehicle control (mean ± SEM) from three separate experiments. Representative Western blotting membranes were shown at the bottom; β-actin was used as the loading control. *, $P < 0.05$ *vs.* vehicle control.

trol for that time point (Fig. 2B, a–c, G_0/G_1 phase, S phase, G_2/M phase, respectively). P_4 promoted rNPC exit of G_0/G_1 phase at 4 h (Fig. 2Ba, 70.2 ± 10.6% of vehicle, $P < 0.05$), induced a significant increase in cellular entry into S phase beginning at 6 h (218.6 ± 36.2% of vehicle, $P < 0.05$) and extended until 8 h with a return to baseline at 9 h (Fig. 2Bb). Parallel to the decrease in S phase population, a synchronized increase in G_2/M phase population was observed at 8 h (124.3 ± 15.2% of vehicle, $P < 0.01$), which ceased by 24 h. No statistically significant differences were observed between the control group and P_4-treated group at 24–72 h in G_0/G_1, S, or G_2/M phase populations.

Results of the FACS analysis confirmed the BrdU dose-response data, indicating that at 100 pM P_4 is a potent mitotic agent in rNPCs. The timely coordinated changes in the G_0/G_1, S, and G_2/M phase populations indicated that P_4 induced rNPC entrance and completion of a full cell cycle. P_4 induced a 1-fold increase in the S-phase population and a subsequent 24.3 ± 15.2% increase in the M-phase population, indicating that only a portion of the S-phase population cells passed the S/M checkpoint and to give rise to new cells. Moreover, the amplitude in the change of the M-phase populations is consistent with results from previous BrdU dose-response experiment, where 100 pM P_4 induced a 23.5 ± 1.6% increase in BrdU incorporation (Fig. 2A).

P_4 regulates gene expression of cell-cycle proteins

P_4-induced proliferation predicted its regulation of rNPC cell cycle gene expression. To determine P_4 regulation of cell cycle gene expression, RNA was extracted from rNPCs after 6 h P_4 exposure and processed for analysis of genes known to control cell proliferation. The 6-h time point was selected based on previous FACS results because it was the time when rNPCs exhibited the most robust increase in the S-phase cell population. Gene array analyses indicated that at the mRNA level, P_4 induced a significant up-regulation of genes that promote progression through the cell cycle and simultaneously decrease expression of the cell cycle inhibitor genes (Fig. 3A). Robust increases occurred in genes that promote cell cycle progression, such as a 2-fold increase in cyclin-dependent kinase (CDK)-4 (promotes G_1 phase progression) and CDK2 (promotes G_1/S phase progression), a 3-fold increase in cyclin A (promotes S/M phase transition), and more than a 2-fold increase in Cdc2, cyclin G1 and -2, and cyclin B (promote G_2/M phase progression). In contrast, expression of inhibitors of cell cycle progression, such as CDKn2b, CDKn3, and Wee1, was significantly decreased. Several well-defined cell proliferation markers (37), including

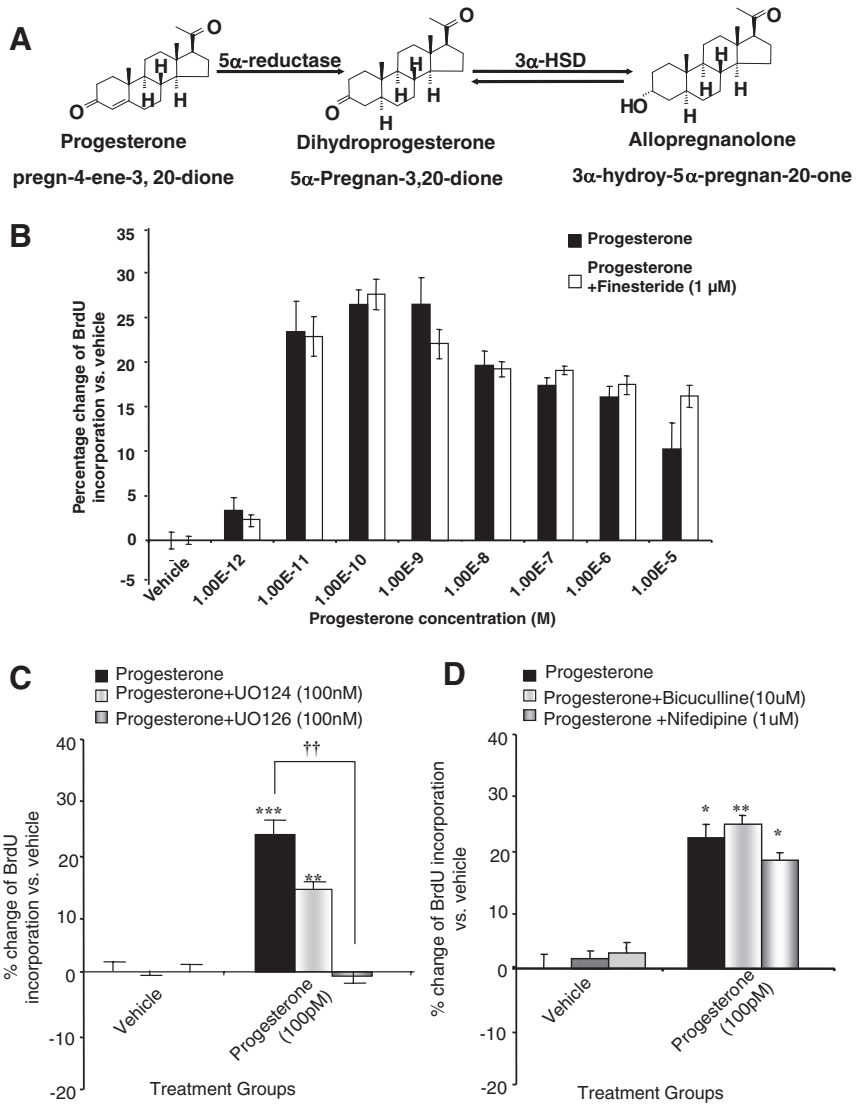

FIG. 4. P_4-induced proliferation of rNPC is independent of its metabolites and requires ERK signaling. A, Pathway showing conversion of P_4 to its metabolites and required enzymes. B, Rat NPCs were starved for 4–6 h and then treated with 100 pM P_4 alone or 100 pM P_4+finestaride for 24 h. Rat NPC proliferation was evaluated by BrdU chemiluminescence ELISA measuring BrdU incorporation. Comparative analysis showed no statistical significant difference between the P_4-alone and P_4+finesteride group. Data were collected from at least three independent experiments and plotted as percentage increase of BrdU incorporation in the P_4-treated rNPCs *vs.* vehicle control (mean ± SEM). C, Rat NPCs were starved for 4–6 h and treated with 100 pM P_4 alone or in combination of ERK inhibitor UO126 or in combination of the inactive analog of UO126 (UO124). After 24 h rNPC proliferation was evaluated by BrdU chemiluminescence ELISA measuring BrdU incorporation. P_4-induced cell proliferation could be totally abolished by ERK inhibitor UO126, and UO124 did not show significant effect. Data were collected from five independent experiments and plotted as percentage increase of BrdU incorporation *vs.* vehicle control (mean ± SEM). **, $P < 0.01$ *vs.* vehicle control; ***, $P < 0.001$ *vs.* vehicle control; ††, $P < 0.01$ P_4 alone *vs.* P_4+UO126. D, Rat NPCs were starved for 4–6 h and treated with 100 pM P_4 alone or in combination of $GABA_A$ receptor antagonist bicuculline or in combination of L-type calcium channel blocker nifedipine. After 24 h rNPC proliferation was evaluated by BrdU chemiluminescence ELISA measuring BrdU incorporation. The proliferative effect of P_4 was not blocked by bicuculline or nifedipine. Data were collected from three independent experiments and plotted as percentage increase of BrdU incorporation *vs.* vehicle control (mean ± SEM). *, $P < 0.05$ *vs.* control; **, $P < 0.01$ *vs.* control.

Mcm5, Mcm7, and PCNA, showed a nearly 2-fold increase in expression. Furthermore, the gene expression data were divided into subgroups of genes known to promote or inhibit cell proliferation, and the data from each subgroup of genes were subjected to multivariate ANOVA (37). Results of this analysis indicated a statistically significant effect of P_4 treatment on cyclins, CDKs, and CDK inhibitors (supplemental Table 1, published as supplemental data on The Endocrine Society's Journals Online web site at http://endo.endojournals.org).

Gene array results were further validated by real-time PCR (Fig. 3B) and Western blot analyses (Fig. 3C). Real-time PCR was performed for five mRNAs coding for genes that promote transitions through the cell cycle, two genes that inhibit cell cycle progression, and two invariant genes. P_4 increased the mRNA expression level of cyclin A, cyclin B, PCNA, and Cdc2 and decreased the mRNA expression of Cdkn2c and Cdkn3 at magnitudes comparable with the gene array data. Western blot analyses indicated that P_4 increased PCNA and CDC2 protein level by 62.9 ± 11.8 and 28.9 ± 6.4%, respectively ($P < 0.05$ *vs.* vehicle), an effect comparable with that induced by bFGF (90.7 ± 17.2 and 35.3 ± 15.7%, respectively, $P < 0.05$ *vs.* vehicle). Together, these data indicated that P_4 promoted the expression of activators of cell-cycle progression, such as cyclins, CDKs, and PCNA and simultaneously down-regulating the CDK inhibitors. Moreover, S/M phase regulatory genes exhibited the most robust changes and confirmed results from previous FACS analysis, where 6 h was demonstrated to be the time point when S phase populations peak.

P_4-induced proliferation of rNPCs is independent of its metabolites and requires ERK signaling

Based on previous findings from our group and others (34, 38, 39), P_4 and its metabolites can act as mitotic agents. To determine whether P_4 metabolites contributed to or were required for P_4-induced increase in proliferation, rNPCs were simultaneously exposed to P_4 and finasteride, which at nanomolar range effectively blocks the conversion of P_4 to 5α-dihydroprogesterone and APα (40) (Fig. 4A). The concentration of finasteride was selected based on our previous investigation that 1 μM was the maximally effective dose for inhibition of P_4 conversion without inducing inhibition of cell proliferation and/or cell death. Results from BrdU ELISA indicated no statistically significant difference between the P_4 alone and P_4 plus finasteride group at 24 h (Fig. 4B), indicating that the proliferative effect of P_4 is not dependent on metabolism to its metabolites.

Our group earlier reported that P_4 activates the ERK signaling pathway to mediate its neuroprotective actions (27), whereas APα increased proliferation through activation of the γ-aminobutyric acid $(GABA)_A$ receptor and L-type Ca^{2+}

channel (34). To determine the signaling pathway required for P_4-induced proliferation, BrdU ELISA was carried out in rNPCs exposed to pharmacological agents to interrogate the ERK and Ca^{2+}-dependent systems. At 24 h, P_4 induced a cumulative increase of 26.3 ± 1.6% ($P < 0.001$ *vs.* vehicle) in rNPC proliferation, an effect that was abolished by the ERK inhibitor UO126 and not significantly affected by the same dose of the inactive analog of UO124 ($P = 0.17$) (Fig. 4C). Application of neither bicuculline ($GABA_A$ receptor antagonist) nor nifedipine (L-type Ca^{2+} channel blocker) inhibited P_4-induced rNPC proliferation (Fig. 5D). Together, results of these analyses indicate that P_4-induced rNPC proliferation is dependent on the ERK signaling pathway.

The proliferative effect of progesterone is independent of cPR binding affinity

To determine the structure and activity relationship for P_4-induced rNPC proliferation, BrdU ELISA was used to compare the proliferative effects of P_4 and its structural analogs at the same concentrations (Fig. 5A). Results indicated that at 24 h, P_4, APα, and ganaxolone were equally efficacious at their EC_{100} concentrations, with EC_{100} values being $1 \times e^{-10}$ M, $1 \times e^{-8}$, and $1 \times e^{-5}$ M, respectively. Epiallopregnanolone exhibited moderate proliferative efficacy, whereas epipregnanolone, allopregnanetriol, pregnanolone sulfate, 5α-dihydroprogesterone, and 5α-pregnan-3β-ol were ineffective. Additionally, allopregnandiol induced a significant decrease in BrdU incorporation in a dose-dependent manner, consistent with its effect on rNPC differentiation (34). APα, epiallopregnanolone, and epipregnanolone are three molecules that differ in the position of the 3-hydroxyl and 5-hydrogen groups. Change in one or both α-positioned group(s) to the β-position results in a decrease in the proliferative efficacy (epiallopregnanolone) and eventually resulting in ineffectiveness (epipregnanolone). Computational modeling revealed three critical structural features: the 18th ketone group position, the α-positioned fifth hydrogen, and the at the third hydroxyl group (Fig. 5B). Importantly, these structural features matched with the binding features required for PGRMC1 (41).

A parallel computational modeling of the binding modes of tested molecules with cPR, together with a fluorescent polarization competitive cPR binding assay, indicated that there is no clear association between the binding affinity to cPR and proliferative capabilities of these neurosteroids (see supplemental Table 2). Collectively, these data indicated no clear link between cPR activation and rNPC proliferation.

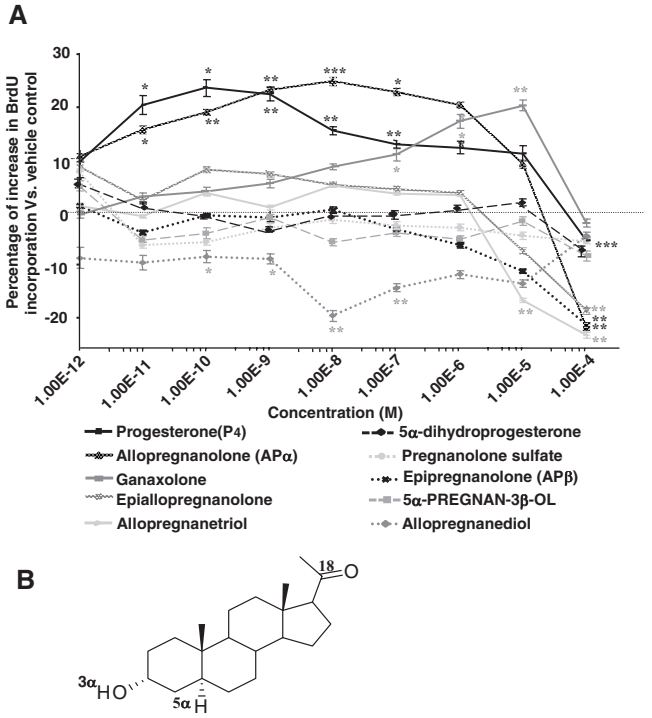

FIG. 5. The proliferative effect of P_4 is independent of cPR binding affinity. Rat NPCs were starved for 4 h before treatment of P_4 and its analogs ($1 \times e^{-12}$ to $1 \times e^{-4}$ M) for 24 h, and cell proliferation was evaluated by BrdU chemiluminescence ELISA measuring BrdU incorporation. Ethanol was used as vehicle control ($1 \times e^{-6}$). A, P_4 and its structural analogs exhibited varied effects on rNPC proliferation. P_4, APα, and ganaxolone were equally efficacious and epiallopregnanolone exhibited moderate proliferative effect. Epipregnanolone, allopregnanetriol, pregnanolone sulfate, 5α-dihydroprogesterone, and 5α-pregnan-3β-ol were ineffective, whereas allopregnandiol induced a significant decrease in BrdU incorporation. Data were collected from three independent assays, analyzed using one-way ANOVA, followed by Neuman-Keuls *post hoc* test, and plotted as percentage increase *vs.* vehicle control (mean ± SEM). *, $P < 0.05$ *vs.* vehicle control; **, $P < 0.01$ *vs.* vehicle control; ***, $P < 0.005$ *vs.* vehicle control. B, Structure activity relationship analysis of the proliferative ability of the steroids and their binding affinity to cPR. Results were collected from three independent PR-binding assays and summarized in supplemental Table 2. As highlighted in the chemical structure of APα, three structural features were revealed to be critical for P_4 and its analog-induced proliferation in rNPCs: the ketone group at the 18 position, the α-positioned hydrogen at the 5 position, and the hydroxyl group at the 3 position.

PRGMC1 is necessary and sufficient for P4-induced rNPC proliferation

Evidence so far has excluded the potential role of cPR in mediating P_4-induced cell proliferation, leaving PGRMC1 as a possible candidate. To determine the correlation between PGRMC1 and rNPC proliferation, double labeling of PGRMC1 and PCNA was conducted in rNPCs 10–12 h after P_4 treatment. Immunocytochemical analysis revealed a subpopulation of PGRMC1-positive rNPCs (Fig. 6A). Furthermore, only PGRMC1-positive cells were PCNA positive after P_4 exposure (Fig. 6A), indicating that PGRMC1 was correlated with P_4-induced rNPC proliferation.

To further determine whether PGRMC1 was required for P_4-induced proliferation, siRNA was introduced to knock down PGRMC1 expression in the rNPCs. Among all the siRNAs tested, PGRMC1 siRNA 253163 was determined to be most efficient, with a 68.1 ± 3.0% ($P < 0.05$ *vs.* vehicle) knockdown rate compared with scrambled siRNA control (Fig. 6B-II). Knockdown of PGRMC1 had no effect on the basal level proliferation in rNPCs under maintenance condition when bFGF is present (28, 29), as demonstrated by the constant PCNA and CDC2 protein expression across treatment groups (Fig. 6B, II and III). To assess the effect of PGRMC1 depletion, rNPCs were treated with either scrambled or PGRMC1 siRNA. After 48 h, rNPCs were treated with bFGF, vehicle, or P_4 and the ability of P_4 to promote proliferation was determined by PCNA and CDC2 protein expression level. In response to P_4, PCNA and CDC2 expression increased by 63.9 ± 20.8 and 37.5 ± 7.6%,

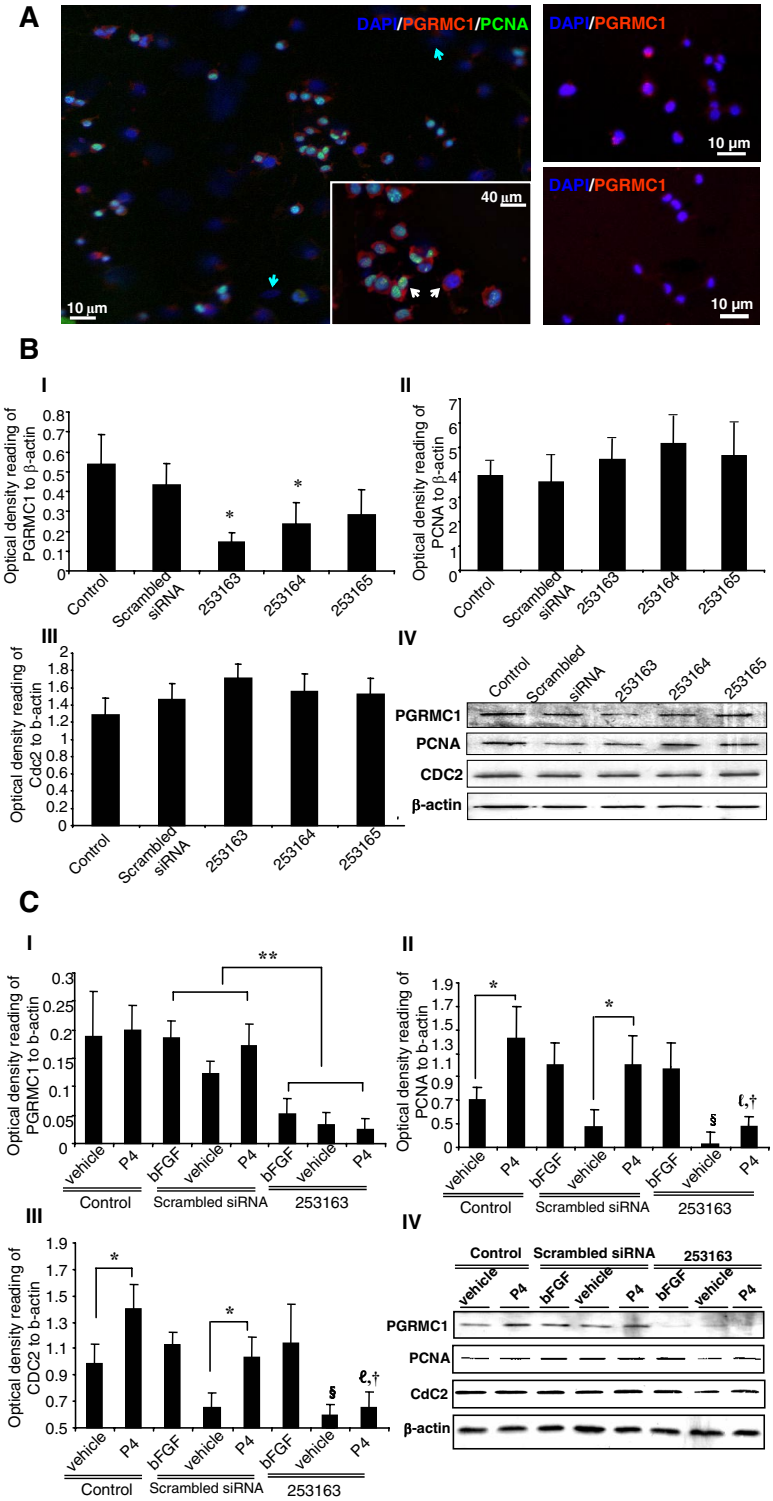

FIG. 6. PGRMC1 is critical for P_4-induced rNPC proliferation. siRNA against PGRMC1 was introduced to rNPCs to determine the correlation between PGRMC1 and cell proliferation. A, *left panel*, rNPCs were exposed to P_4 for 10–12 h and processed for immunostaining for PGRMC1 and PCNA. PGRMC1 was expressed in selected population of rNPCs (*blue arrows* showing rNPCs that were PGRMC1 negative). PCNA-positive cells can be found only in PGRMC1-positive cells (*inserted image*, *white arrows*). *Right panel*, Immunostaining for PGRMC1 expression in rNPCs before (*top panel*) and after (*bottom panel*) 48 h PGRMC1 siRNA 253163 treatment. B, The effect of scramble and three different PGRMC1 siRNAs on the expression of PGRMC1 (B, I) and mitotic markers PCNA (B, II) and CDC2 (B, III). Representative Western blotting membranes were shown (B, IV); β-actin was used as loading control. Rat NPCs were exposed to siRNA for 48 h and processed for Western blot analysis. Results were collected from three independent experiments and plotted as OD ratio to β-actin (mean ± SEM). *, $P < 0.05$ *vs.* scramble control. C, The effect of scramble and PGRMC1 siRNA 253163 on P_4-induced mitotic marker expression. After 48 h siRNA treatment, rNPCs were exposed to bFGF, vehicle control (ethanol), and P_4 respectively ($P < 0.05$ *vs.* vehicle). Introduction of siRNA against PGRMC1 resulted in a 59.7 and 84.0% decrease in P_4-induced PCNA and CDC2 expression compared with the scrambled siRNA-treated group (Fig. 6C II and III, $P < 0.05$). Notably, knockdown of PGRMC1 remarkably decreased basal expression level of PCNA and CDC2 mitotic markers in rNPCs (Fig. 6C, II and III, $P < 0.05$), suggesting that PGRMC1 could be involved in signaling pathways regulating constitutive proliferation in rNPCs. These results further confirmed that knockdown of PGRMC1 specifically and significantly decreased P_4-induced rNPC proliferation. Collectively, these data demonstrated that PGRMC1 is necessary and sufficient for P_4-induced rNPC proliferation.

Discussion

Results of the present study demonstrate for the first time that P_4 increases proliferation of adult rNPCs in a dose-dependent manner. P_4 significantly increased the expression of genes required for progression through the cell cycle and inhibited expression of genes involved in cell cycle repression. Mechanistic analyses revealed that rNPC proliferation was a direct effect of P_4 and not exerted via its metabolites. Furthermore, P_4-induced rNPC proliferation is dependent on the ERK/MAPK signaling pathway and is mediated by the membrane PR, PGMRC1.

P_4 increased proliferation of rNPC from female adult rat hippocampus with maximal proliferative efficacy within the picomolar/nanomolar range, which was reversed at higher micromolar range. In adult female rat, P_4 plasma levels range from 1 to 200 nM, and the concentration of P_4 in the brain is thought to closely follow circulating plasma levels (42, 43). The effective concentration of P_4 is comparable with that of both plasma and brain, indicating the physiological relevance of P_4's mitotic effect. Other groups have reported that P_4 regulates cell proliferation in both peripheral and central nervous system at nanomolar/micromolar ranges (17, 18, 20). The discrepancies between the effective P_4 concentrations across studies may arise from varied P_4 responsiveness in different cell and tissue types. Indeed, hippocampal cells are more sensitive than cerebellum cells in response to P_4-induced neuroprotective effects, with minimally effective

concentrations within the nanomolar to micromolar range, respectively (1). Alternatively, P_4 may promote cell proliferation via different signaling pathways (1) as well as conversion to its metabolites (38), leading to the different requirements in P_4 concentrations.

The mitotic efficacy of P_4 was comparable to bFGF as evidenced by BrdU incorporation and regulation of the expression PCNA and CDC2, two well-defined and commonly used markers for cell proliferation (44). PCNA is a marker for cells in early G_1/S phase of the cell cycle and acts as a homotrimer to increase the processing of leading strand synthesis during DNA replication. CDC2/CDK1 is the catalytic subunit of the protein kinase complex M-phase promoting factor and is required for the G_2/M phase transition (44). Both PCNA and CDC2 expression were up-regulated after P_4 treatment, indicating that P_4 promoted rNPC entry into and completion of the cell cycle. Importantly, FACS analysis indicated that P_4-induced DNA synthesis did not persist beyond 24 h, indicating that P_4-responsive rNPCs traversed the cell cycle but did not remain in a proliferative state and thus P_4, *in vitro*, did not induce prolonged or uncontrolled proliferation. P_4 may increase proliferation by speeding up cell cycle in the same cell population or recruiting more cells into cell cycle. Immunocytochemical analyses argued for the latter because only PGMRC1+rNPCs entered into Gs as a result of P_4 exposure; however, the possibility of accelerated cell cycle cannot be ruled out at this point.

We previously demonstrated that APα increased NPC proliferation at an optimal dose of 100 nM (34), whereas in the present study, P_4 exhibited an optimal concentration 1000 times lower than that of APα. It was thus unlikely that P_4 promoted proliferation via its metabolites. This was confirmed by application of finasteride, which showed no significant effect on P_4's action. However, recent studies from other groups suggested an effect of P_4 metabolites (39, 45). The discrepancy may due to the differences between embryonic NPCs and adult NPCs because polysialic acid neural cell adhesion molecule-positive progenitors were obtained from postnatal d 1 rat (45). The signaling machinery for P_4 and APα may be differently expressed in embryonic *vs.* adult NPCs. Alternatively, differences may arise from targeting neuronal *vs.* glial progenitor cells. The rNPCs are proneurogenesis have an increasing proportion of neuronal-like cells in long-term cultures (>200 d *in vitro*) (46), whereas the prostate-specific antigen-neural cell adhesion molecule-positive-positive progenitors have a default differentiation to glial lineages (45), and their proliferation may be more relevant to gliogenesis. Although P_4 and APα may be present at the same time in NPCs as evidenced by the presence of 5α-reductase (47), it is possible that they exhibit distinct binding kinetics to their targets and exert effects at different time points.

Although cPR has been reported to respond to P_4 in a nongenomic fashion via activating second messenger signaling cascades (26, 27, 48), results from RT-PCR, steroid specificity analysis, and computational modeling ruled out its involvement in P_4-induced proliferation. Specifically the potent cPR agonist, 5α-dihydroprogesterone and epipregnanolone (49), showed no effect on rNPC proliferation. In fact, multiple groups have reported P_4 effects in the CNS of cPR knockout mice (50), pointing to the involvement of other receptors in response to P_4. PRGMC1 is reported to mediate the response to P_4 in murine embryonic sensory neurons (51), granulose cells (33), and neonatal rat Purkinje cells (52), suggested to play a role in promoting neonatal dendritic growth, spinogenesis, and synaptogenesis. Our study indicated that siRNA-induced depletion of PGRMC1 significantly and specifically reduced P_4-increased cell proliferation. These findings together with the computational modeling analyses indicated that PGRMC1 was the key mediator of P_4-induced rNPC proliferation. siRNA depletion of PGRMC1 was not absolute and left a residual 31.8% expression and thus could explain the residual P_4 induction of proliferation markers. Alternatively, other P_4-binding receptors such as the seven-transmembrane domain-β (1) could account for the residual P_4-induced proliferation, although expression of such receptors has not been documented in rNPCs. Knockdown of PGRMC1 significantly decreased basal expression level of mitotic markers in rNPCs, indicating that P_4 requires PGRMC1 to induced proliferation, whereas PGRMC1 may respond to factors other than P_4 to regulate rNPC proliferation. Indeed, PGRMC1 has been shown to be activated by heme and steroid/sterol ligands and SH2- and SH3-domain proteins as well as kinases, implicating a possible function for PGRMC1 in regulating protein interactions and intracellular signal transduction (1, 53), which may be crucial for proliferation.

The underlying mechanism for the correlation between elevated expression of PGRMC1 and cell proliferation remains unclear. One potential explanation is the neurotrophic activity of the secreted PGRMC1 family member neudesin, which directly stimulates MAPK and Akt signaling to promote proliferation and neuronal differentiation in mouse NPCs (54, 55). Our results indicating that P_4-induced, PGRMC1-dependent cell proliferation required ERK signaling pathway are consistent with these earlier findings suggesting that P_4-induced proliferation via the ERK signaling pathway generalizes to other cell systems.

P_4 is well known for its neuroprotective effects within the CNS and has been used as a myelinating agent and as a treatment for traumatic brain (4). In the aged brain, both the pool of neural stem cells and their proliferative potential are markedly diminished (56–58). The discovery that P_4 could promote adult rNPC proliferation highlights the potential use of P_4 as a regenerative agent in adult brain. Indeed, several studies report that administration of P_4 could improve cognitive performance in the aging mouse when compared with control groups (59–61). Together with our present data, these findings suggest a promising strategy for promoting neurogenesis in the adult brain. Furthermore, the finding that estrogen receptor and PGRMC1 were mutually exclusive in breast tumor sections, and PGRMC1 labeling increased in hypoxic areas of the tumor (62, 63) suggests that

FIG. 6 (cont). for 10–12 h and processed for Western blot analysis. PGRMC1 siRNA significantly and specifically reduced the expression of PGRMC1 (C, I), blocked the increase of PCNA (C, II) and CDC2 (C, III) in response to P_4, and had no significant effect on bFGF-induced mitotic marker expression. Representative Western blotting membranes were shown (C, IV); β-actin was used as loading control. Results were collected from three independent experiments and plotted as percent increase *vs.* vehicle control (mean ± SEM). *, $P < 0.05$; **, $P < 0.01$; §, $P < 0.05$ between vehicle control in the control group and PGRMC1 siRNA 253163 group; ℓ, $P < 0.05$ *vs.* P_4 treatment in scramble control group; †, $P < 0.05$ *vs.* bFGF treatment in PGRMC1 siRNA 253163 group.

targeting PGMRC1 may be a novel approach to promote proliferation in brain and avoid tumorogenic effects in estrogen receptor-positive cells.

Acknowledgments

We thank Dr. Fred Gage (Salk Institute, La Jolla, California) for the gift of adult rat neural progenitor cells. Drs. Martin Wehling and Alexandra Wendler (University of Heidelberg-Mannheim, Heidelberg, Maybachstr. 14, D-68169 Mannheim, Germany) for providing the NT-PGRMC1 antibody, and Dr. Peluso (University of Connecticut Health Center, Farmington, CT) for technical counsel regarding PGRMC1 antibody. The authors thank Jia Yao and Dr. Ronald Irwin for their contributions.

Address all correspondence and requests for reprints to: Roberta Diaz Brinton, Ph.D., Department of Pharmacology and Pharmaceutical Sciences, University of Southern California, School of Pharmacy, 1985 Zonal Avenue, Los Angeles, California 90089. E-mail: rbrinton@usc.edu.

This work was supported by National Institute on Aging Grant 1 PO1 AG026572, Project 3 of Progesterone in Brain Aging and Alzheimer's Disease Program Project (to R.D.B.).

Current address for J.W.: University of Mississippi Medical Center, 2500 North State Street, Jackson, Mississippi 39216. E-mail: jwang@pathology.umsmed.edu.

Current address for J.N.: Amgen. Inc., 1 Amgen Center Drive, Thousand Oaks, California 91320. E-mail: jnilsen@amgen.com.

Disclosure Summary: L.L., J.W., L.Z., K.M., and K.W. have nothing to declare. J.N. is currently employed by Amgen and was a University of Southern California faculty member at the time the experiments were conducted. R.D.B. has previously consulted for Wyeth Research.

References

1. **Brinton RD, Thompson RF, Foy MR, Baudry M, Wang J, Finch CE, Morgan TE, Pike CJ, Mack WJ, Stanczyk FZ, Nilsen J** 2008 Progesterone receptors: form and function in brain. Front Neuroendocrinol 29:313–339
2. **Baulieu E, Schumacher M** 2000 Progesterone as a neuroactive neurosteroid, with special reference to the effect of progesterone on myelination. Steroids 65:605–612
3. **Irwin RW, Yao J, Hamilton RT, Cadenas E, Brinton RD, Nilsen J** 2008 Progesterone and estrogen regulate oxidative metabolism in brain mitochondria. Endocrinology 149:3167–3175
4. **Stein DG** 2001 Brain damage, sex hormones and recovery: a new role for progesterone and estrogen? Trends Neurosci 24:386–391
5. **Schumacher M, Guennoun R, Stein DG, De Nicola AF** 2007 Progesterone: therapeutic opportunities for neuroprotection and myelin repair. Pharmacol Ther 116:77–106
6. **Wong AM, Rozovsky I, Arimoto JM, Du Y, Wei M, Morgan TE, Finch CE** 2009 Progesterone influence on neurite outgrowth involves microglia. Endocrinology 150:324–332
7. **Melcangi RC, Magnaghi V, Martini L** 1999 Steroid metabolism and effects in central and peripheral glial cells. J Neurobiol 40:471–483
8. **Baulieu EE, Robel P, Schumacher M** 2001 Neurosteroids: beginning of the story. Int Rev Neurobiol 46:1–32
9. **Mellon SH, Griffin LD** 2002 Neurosteroids: biochemistry and clinical significance. Trends Endocrinol Metab 13:35–43
10. **Lauber ME, Lichtensteiger W** 1996 Ontogeny of 5α-reductase (type 1) messenger ribonucleic acid expression in rat brain: early presence in germinal zones. Endocrinology 137:2718–2730
11. **Schumacher M, Guennoun R, Robert F, Carelli C, Gago N, Ghoumari A, Gonzalez Deniselle MC, Gonzalez SL, Ibanez C, Labombarda F, Coirini H, Baulieu EE, De Nicola AF** 2004 Local synthesis and dual actions of progesterone in the nervous system: neuroprotection and myelination. Growth Horm IGF Res 14(Suppl A):S18–S33
12. **Pomata PE, Colman-Lerner AA, Baranao JL, Fiszman ML** 2000 *In vivo* evidences of early neurosteroid synthesis in the developing rat central nervous system and placenta. Brain Res Dev Brain Res 120:83–86
13. **Bernstein L** 2002 Epidemiology of endocrine-related risk factors for breast cancer. J Mammary Gland Biol Neoplasia 7:3–15
14. **Chlebowski RT, Hendrix SL, Langer RD, Stefanick ML, Gass M, Lane D, Rodabough RJ, Gilligan MA, Cyr MG, Thomson CA, Khandekar J, Petrovitch H, McTiernan A** 2003 Influence of estrogen plus progestin on breast cancer and mammography in healthy postmenopausal women: the Women's Health Initiative Randomized Trial. JAMA 289:3243–3253
15. **Kiss R, Paridaens RJ, Heuson JC, Danguy AJ** 1986 Effect of progesterone on cell proliferation in the MXT mouse hormone-sensitive mammary neoplasm. J Natl Cancer Inst 77:173–178
16. **Pike MC, Ross RK** 2000 Progestins and menopause: epidemiological studies of risks of endometrial and breast cancer. Steroids 65:659–664
17. **Magnaghi V, Ballabio M, Roglio I, Melcangi RC** 2007 Progesterone derivatives increase expression of Krox-20 and Sox-10 in rat Schwann cells. J Mol Neurosci 31:149–157
18. **Svenningsen AF, Kanje M** 1999 Estrogen and progesterone stimulate Schwann cell proliferation in a sex- and age-dependent manner. J Neurosci Res 57:124–130
19. **Ghoumari AM, Baulieu EE, Schumacher M** 2005 Progesterone increases oligodendroglial cell proliferation in rat cerebellar slice cultures. Neuroscience 135:47–58
20. **Marin-Husstege M, Muggironi M, Raban D, Skoff RP, Casaccia-Bonnefil P** 2004 Oligodendrocyte progenitor proliferation and maturation is differentially regulated by male and female sex steroid hormones. Dev Neurosci 26:245–254
21. **Tanapat P, Hastings NB, Gould E** 2005 Ovarian steroids influence cell proliferation in the dentate gyrus of the adult female rat in a dose- and time-dependent manner. J Comp Neurol 481:252–265
22. **Baulieu EE, Schumacher M, Koenig H, Jung-Testas I, Akwa Y** 1996 Progesterone as a neurosteroid: actions within the nervous system. Cell Mol Neurobiol 16:143–154
23. **Gonzalez Deniselle MC, Garay L, Gonzalez S, Saravia F, Labombarda F, Guennoun R, Schumacher M, De Nicola AF** 2007 Progesterone modulates brain-derived neurotrophic factor and choline acetyltransferase in degenerating Wobbler motoneurons. Exp Neurol 203:406–414
24. **He J, Evans CO, Hoffman SW, Oyesiku NM, Stein DG** 2004 Progesterone and allopregnanolone reduce inflammatory cytokines after traumatic brain injury. Exp Neurol 189:404–412
25. **Leonelli E, Bianchi R, Cavaletti G, Caruso D, Crippa D, Garcia-Segura LM, Lauria G, Magnaghi V, Roglio I, Melcangi RC** 2007 Progesterone and its derivatives are neuroprotective agents in experimental diabetic neuropathy: a multimodal analysis. Neuroscience 144:1293–1304
26. **Nilsen J, Brinton RD** 2002 Impact of progestins on estrogen-induced neuroprotection: synergy by progesterone and 19-norprogesterone and antagonism by medroxyprogesterone acetate. Endocrinology 143:205–212
27. **Nilsen J, Brinton RD** 2003 Divergent impact of progesterone and medroxyprogesterone acetate (Provera) on nuclear mitogen-activated protein kinase signaling. Proc Natl Acad Sci USA 100:10506–10511
28. **Palmer TD, Markakis EA, Willhoite AR, Safar F, Gage FH** 1999 Fibroblast growth factor-2 activates a latent neurogenic program in neural stem cells from diverse regions of the adult CNS. J Neurosci 19:8487–8497
29. **Ray J, Peterson DA, Schinstine M, Gage FH** 1993 Proliferation, differentiation, and long-term culture of primary hippocampal neurons. Proc Natl Acad Sci USA 90:3602–3606
30. **Doetsch F, García-Verdugo JM, Alvarez-Buylla A** 1997 Cellular composition and three-dimensional organization of the subventricular germinal zone in the adult mammalian brain. J Neurosci 17:5046–5061
31. **Romero-Ramos M, Vourc'h P, Young HE, Lucas PA, Wu Y, Chivatakarn O, Zaman R, Dunkelman N, el-Kalay MA, Chesselet MF** 2002 Neuronal differentiation of stem cells isolated from adult muscle. J Neurosci Res 69:894–907
32. **Peluso JJ, Pappalardo A, Losel R, Wehling M** 2006 Progesterone membrane receptor component 1 expression in the immature rat ovary and its role in mediating progesterone's antiapoptotic action. Endocrinology 147:3133–3140
33. **Peluso JJ, Romak J, Liu X** 2008 Progesterone receptor membrane component-1 (PGRMC1) is the mediator of progesterone's antiapoptotic action in spontaneously immortalized granulosa cells as revealed by PGRMC1 small interfering ribonucleic acid treatment and functional analysis of PGRMC1 mutations. Endocrinology 149:534–543
34. **Wang JM, Johnston PB, Ball BG, Brinton RD** 2005 The neurosteroid allopregnanolone promotes proliferation of rodent and human neural progenitor cells and regulates cell-cycle gene and protein expression. J Neurosci 25:4706–4718

35. **Wang JM, Liu L, Irwin RW, Chen S, Brinton RD** 2008 Regenerative potential of allopregnanolone. Brain Res Rev 57:398–409
36. **Sierra A, Gottfried-Blackmore A, Milner TA, McEwen BS, Bulloch K** 2008 Steroid hormone receptor expression and function in microglia. Glia 56:659–674
37. **Gannon JV, Nebreda A, Goodger NM, Morgan PR, Hunt T** 1998 A measure of the mitotic index: studies of the abundance and half-life of p34cdc2 in cultured cells and normal and neoplastic tissues. Genes Cells 3:17–27
38. **Gago N, Akwa Y, Sananès N, Guennoun R, Baulieu EE, El-Etr M, Schumacher M** 2001 Progesterone and the oligodendroglial lineage: stage-dependent biosynthesis and metabolism. Glia 36:295–308
39. **Giachino C, Galbiati M, Fasolo A, Peretto P, Melcangi RC** 2004 Effects of progesterone derivatives, dihydroprogesterone and tetrahydroprogesterone, on the subependymal layer of the adult rat. J Neurobiol 58:493–502
40. **Kenny B, Ballard S, Blagg J, Fox D** 1997 Pharmacological options in the treatment of benign prostatic hyperplasia. J Med Chem 40:1293–1315
41. **Falkenstein E, Eisen C, Schmieding K, Krautkramer M, Stein C, Losel R, Wehling M** 2001 Chemical modification and structural analysis of the progesterone membrane binding protein from porcine liver membranes. Mol Cell Biochem 218:71–79
42. **Butcher RL, Collins WE, Fugo NW** 1974 Plasma concentration of LH, FSH, prolactin, progesterone and estradiol-17β throughout the 4-day estrous cycle of the rat. Endocrinology 94:1704–1708
43. **Nequin LG, Alvarez J, Schwartz NB** 1979 Measurement of serum steroid and gonadotropin levels and uterine and ovarian variables throughout 4 day and 5 day estrous cycles in the rat. Biol Reprod 20:659–670
44. **Wang JM, Liu L, Brinton RD** 2008 Estradiol-17β-induced human neural progenitor cell proliferation is mediated by an estrogen receptor β-phosphorylated extracellularly regulated kinase pathway. Endocrinology 149:208–218
45. **Gago N, El-Etr M, Sananes N, Cadepond F, Samuel D, Avellana-Adalid V, Baron-Van Evercooren A, Schumacher M** 2004 3α,5α-Tetrahydroprogesterone (allopregnanolone) and γ-aminobutyric acid: autocrine/paracrine interactions in the control of neonatal PSA-NCAM+ progenitor proliferation. J Neurosci Res 78:770–783
46. **Gage FH, Ray J, Fisher LJ** 1995 Isolation, characterization, and use of stem cells from the CNS. Annu Rev Neurosci 18:159–192
47. **Melcangi RC, Froelichsthal P, Martini L, Vescovi AL** 1996 Steroid metabolizing enzymes in pluripotential progenitor central nervous system cells: effect of differentiation and maturation. Neuroscience 72:467–475
48. **Lange CA, Richer JK, Shen T, Horwitz KB** 1998 Convergence of progesterone and epidermal growth factor signaling in breast cancer. Potentiation of mitogen-activated protein kinase pathways. J Biol Chem 273:31308–31316
49. **Schumacher M, Guennoun R, Ghoumari A, Massaad C, Robert F, El-Etr M, Akwa Y, Rajkowski K, Baulieu EE** 2007 Novel perspectives for progesterone in hormone replacement therapy, with special reference to the nervous system. Endocr Rev 28:387–439
50. **Krebs CJ, Jarvis ED, Chan J, Lydon JP, Ogawa S, Pfaff DW** 2000 A membrane-associated progesterone-binding protein, 25-Dx, is regulated by progesterone in brain regions involved in female reproductive behaviors. Proc Natl Acad Sci USA 97:12816–12821
51. **Viero C, Mechaly I, Aptel H, Puech S, Valmier J, Bancel F, Dayanithi G** 2006 Rapid inhibition of Ca2+ influx by neurosteroids in murine embryonic sensory neurones. Cell Calcium 40:383–391
52. **Sakamoto H, Ukena K, Takemori H, Okamoto M, Kawata M, Tsutsui K** 2004 Expression and localization of 25-Dx, a membrane-associated putative progesterone-binding protein, in the developing Purkinje cell. Neuroscience 126:325–334
53. **Cahill MA** 2007 Progesterone receptor membrane component 1: an integrative review. J Steroid Biochem Mol Biol 105:16–36
54. **Kimura I, Nakayama Y, Yamauchi H, Konishi M, Miyake A, Mori M, Ohta M, Itoh N, Fujimoto M** 2008 Neurotrophic activity of neudesin, a novel extracellular heme-binding protein, is dependent on the binding of heme to its cytochrome b5-like heme/steroid-binding domain. J Biol Chem 283:4323–4331
55. **Kimura I, Konishi M, Miyake A, Fujimoto M, Itoh N** 2006 Neudesin, a secreted factor, promotes neural cell proliferation and neuronal differentiation in mouse neural precursor cells. J Neurosci Res 83:1415–1424
56. **Jin K, Sun Y, Xie L, Batteur S, Mao XO, Smelick C, Logvinova A, Greenberg DA** 2003 Neurogenesis and aging: FGF-2 and HB-EGF restore neurogenesis in hippocampus and subventricular zone of aged mice. Aging Cell 2:175–183
57. **Wise PM** 2003 Creating new neurons in old brains. Sci Aging Knowledge Environ 2003:PE13
58. **Enwere E, Shingo T, Gregg C, Fujikawa H, Ohta S, Weiss S** 2004 Aging results in reduced epidermal growth factor receptor signaling, diminished olfactory neurogenesis, and deficits in fine olfactory discrimination. J Neurosci 24:8354–8365
59. **Frye CA, Walf AA** 2008 Progesterone enhances performance of aged mice in cortical or hippocampal tasks. Neurosci Lett 437:116–120
60. **Frye CA, Walf AA** 2008 Progesterone to ovariectomized mice enhances cognitive performance in the spontaneous alternation, object recognition, but not placement, water maze, and contextual and cued conditioned fear tasks. Neurobiol Learn Mem 90:171–177
61. **Frye CA, Walf AA** 2008 Effects of progesterone administration and APPswe+PSEN1Δe9 mutation for cognitive performance of mid-aged mice. Neurobiol Learn Mem 89:17–26
62. **Crudden G, Loesel R, Craven RJ** 2005 Overexpression of the cytochrome p450 activator hpr6 (heme-1 domain protein/human progesterone receptor) in tumors. Tumour Biol 26:142–146
63. **Craven RJ** 2008 PGRMC1: a new biomarker for the estrogen receptor in breast cancer. Breast Cancer Res 10:113